FOREX Publication
Open Access | Rapid and quality publishing

International Journal of
Electrical and Electronics Research (IJEER)
Research Article | Volume 11, Issue 4 | Pages 1057-1064 | e-ISSN: 2347-470X

# High-frequency Differential Mode Modeling of Universal Motor's Windings

**Dr. Mohammed Hamza Bermaki[1*], Dr. Houcine Miloudi[2], Dr. Mohamed Miloudi[3], Dr. Abdelkader Gourbi[4] and Prof. Dr. Abdelber Bendaoud[5]**

*[1,2,5]Application of plasma, electrostatics and electromagnetic compatibility laboratory (APELEC), Djilali Liabes University of Sidi Bel-Abbès, Algeria, Faculty of Electrical Engineering, [1]bermaki.hamza@gmail.com, [2]el.houcine@yahoo.fr, [5]babdelber@gmail.com*
*[3]Application of plasma, electrostatics and electromagnetic compatibility laboratory (APELEC), Ahmed Zabana University Center, Relizane, Algeria., mohamed.miloudi@univ-sba.dz*
*[4]Application of plasma, electrostatics and electromagnetic compatibility laboratory (APELEC), Institute of Applied Sciences and Techniques, Ahmed Ben Bella University, Oran, Algeria, Faculty of Science and Technology, aekett@yahoo.fr*

***Correspondence:** Dr. Mohammed Hamza Bermaki; bermaki.hamza@gmail.com, Phone number: +213555411723

**ABSTRACT-** The universal motor is a rotating electrical machine that can operate on either direct current or single-phase alternating current, similar to a DC motor. It has been widely used in various small and inexpensive drives for a long time, mostly in home appliances and hand tools. The noise generated by a universal motor is believed to be closely associated with the electromagnetic torque fluctuations of the machine, which are caused by variations in the current supplied to the motor. The power electronics utilized for controlling the motor's speed are responsible for these current changes. Accurate high-frequency motor models are crucial for reliable electromagnetic interference simulations in motor drive power electronic systems. Research efforts have expanded to explore different realistic configurations that can be used to investigate the electromagnetic compatibility behavior of electrical machines. This study describes a method for predicting the differential mode impedance of universal motor. The behavior of each motor winding has been individually studied through impedance measurements, starting with the armature, followed by the series winding, and finally the inductive compensating winding. The prediction results over a wide frequency range up to 1 MHz are in good agreement with the measurements and enabled us to propose a model circuit for each motor winding.

**Keywords:** Electric machinery; electromagnetic compatibility; frequency analysis; function transfer; modeling.

**ARTICLE INFORMATION**

**Author(s)**: Dr. Mohammed Hamza Bermaki, Dr. Houcine Miloudi, Dr. Mohamed Miloudi, Dr. Abdelkader Gourbi and Prof. Dr. Abdelber Bendaoud;

**Received**: 26/06/2023; **Accepted**: 16/11/2023; **Published**: 30/11/2023;
**e-ISSN**: 2347-470X;
**Paper Id**: IJEER EMS-069;
**Citation:** 10.37391/IJEER.110425
**Webpage-link**:
https://ijeer.forexjournal.co.in/archive/volume-11/ijeer-110425.html



## 1. INTRODUCTION

DC motors are once again attracting a lot of attention as extremely useful devices [1-3]. This renewed interest can be attributed to advancements in solid-state rectifiers, the development of new and exotic magnetic materials, the introduction of electronic control systems, the rise of electric vehicles, the proliferation of computers, and other innovative technologies. Notably, the DC series motor has evolved into the universal motor, capable of operating on both DC and AC power with minimal modifications [4-6].

A universal motor (UM) is a DC machine with series excitation, meaning that the rotor and field winding are connected in series [7, 8]. Because the machine's torque is related to the square of the current, it can be powered by alternating current. Its stator is laminated to prevent eddy currents from forming in all vast metallic surfaces exposed to alternating magnetic fields. The universal motors are employed in equipment that require a lot of torque, like food processors, low-power tools (up to 1200 W), and vacuum cleaners [9, 10]. This type of motor has several advantages, including inexpensive cost, small size, and high speed. However, it still has a low yield [11-13].

Electrical motors are modeled using a variety of mathematical equations and models. These models are used to predict the performance of the motor under different operating conditions. High frequency modeling is an indispensable tool for the study of electrical machines in terms of electromagnetic compatibility (EMC) [14].

Electromagnetic interference (EMI) in electrical motors can be caused by a variety of sources and can cause motors to run slower, overheat, or even fail. The propagation of conducted disturbances occurs in two modes: Differential and Common Modes. Differential Mode (DM) propagation occurs when the disturbance is applied between two conductors, such as between the two wires of a twisted pair. Parasitic components like resistors, inductors, and capacitors can create disturbances that travel through both wires with the same amplitude but in opposite directions [15].

FOREX Publication
Open Access | Rapid and quality publishing
International Journal of Electrical and Electronics Research (IJEER)
Research Article | Volume 11, Issue 4 | Pages 1057-1064 | e-ISSN: 2347-470X

Several techniques have recently been used to various machine kinds. A three-phase high-frequency (HF) induction motor type with six ports coupled in a delta and star, for instance, was proposed by Karakali Vefa et al [16]. To simulate and anticipate radiation emissions, Joomin Park et al. develop a high frequency model for the stator winding of a BLDC motor [17]. In order to analyze EMI, Zhenyu Zhao et al. present a HF induction motor behavior model with a simplified parameterization procedure [18].

The transfer function methodology has been widely used in this sense, providing reliable mathematical models. The transfer function is a useful representation of a linear time invariant dynamical system. Mathematically the transfer function is a function of complex variables. Thus, AC motors have already been studied and modeled with this method giving satisfactory results [19-21].

While universal motors have been the subject of much research, we have found that little has been done to analyze these high-frequency motors. To study EMI, it is necessary to identify their propagation paths, and high-frequency modeling can help to achieve this. In this paper, we have developed a behavioral model based on transfer functions capable of predicting the impedance of universal motor windings in DM for frequencies up to 1MHz. The aims of this work involve the following:

- Develop a mathematical model to represent the DM impedances of the armature, series, and compensation windings, as well as for the universal motor with and without compensation;
- Frequency analysis of DM current propagation paths in universal motors;
- Examine the impact of each winding on the universal motor's EMC performance;
- Propose a model circuit to represent the universal motor windings.

## 2. MATERIALS AND METHODS

We have employed an algorithm based on the transfer function determination to find the impedance of the universal motor windings as a function of frequency. This modeling method's application is based on four steps that need to be properly followed.

*Step1*: Using an impedance analyzer, take practical measurements of the motor windings impedances to be studies over a predetermined frequency range.
*Step2*: From the measurements, identify the resonance frequencies (breakpoints).
*Step3*: Determine the slopes.
*Step4*: Determine the transfer function.

### 2.1 Measurement Setup

The motor being studied is a UM that can operate in both DC and AC voltage. It consists of three windings: the armature, the series winding and the compensating winding. The motor's characteristics are presented in *table 1*.

The measurements in this work were all made using the Wayne Kerr 6500B impedance analyzer, which provides fast and accurate testing of components at frequencies up to 120 MHz. The basic measurement accuracy is ± 0.05%, making this instrument one of the best in its class.

**Table 1: UM characteristics**

| Parameters | Values |
|---|---|
| Voltage | 220 V |
| Mechanical Power | 175 W |
| Full-Load Speed | 1800 RPM |
| Full-Load current | 1.4 A |

Measurements were taken by connecting the motor directly to the impedance analyzer. The wiring diagram is dependent on the windings and propagation mode (common mode or differential mode) being studied. *Figure 1* shows the example of the impedance measurement of the compensating winding in differential mode.

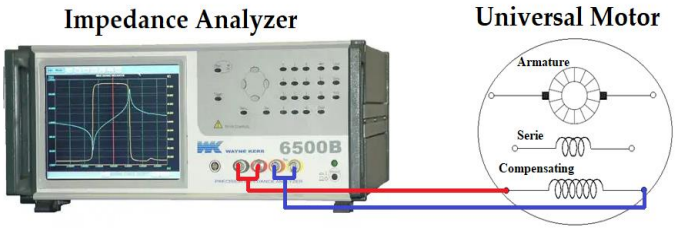


**Figure 1:** DM measurement setup

### 2.2 Frequency Analysis using Transfer Functions

The measurement results allow us to proceed to the next step which is the transfer function modeling. The impedance (magnitude and phase) of each winding has been modeled in DM.

In transfer function modeling, the impedance of motor windings can be represented using a Bode plot. The Bode plot is a graphical representation of the frequency response of a system, showing the magnitude and phase of the transfer function as a function of frequency.

To draw the impedance of motor windings using a Bode plot, it is necessary to typically follow these steps:

- Determine the transfer function of the motor windings: The transfer function relates the output (impedance) to the input (frequency). It is usually expressed in the Laplace domain. The transfer function for the motor windings can be obtained through experimental measurements or derived from the motor's electrical and physical characteristics.
- Convert the transfer function to a frequency response: The transfer function is typically in the Laplace domain, which represents the system's behavior across a range of frequencies. To obtain the frequency response, the transfer function needs to be evaluated at various frequencies.

FOREX Publication
Open Access | Rapid and quality publishing
International Journal of Electrical and Electronics Research (IJEER)
Research Article | Volume 11, Issue 4 | Pages 1057-1064 | e-ISSN: 2347-470X

By plotting the magnitude and phase responses on the Bode plot, you can visualize how the impedance of the motor windings changes with frequency, which provides valuable insights into the motor's behavior and its interaction with the electrical system. It's important to note that the specific shape and characteristics of the Bode plot will depend on the motor's design, the winding configuration, and other electrical parameters.

Transfer functions of first-order and multi-order systems are employed for this purpose. For example, according to *equations (1) and (2)*, the transfer function of a first-order system and a second-order system can be calculated as a function of frequency, respectively:

$$Z_H = k\left(\frac{p}{w_n}+1\right), \quad (1)$$

$$Z_H = \frac{k}{\left[\left(\frac{1}{w_n^2}\right)p^2+\frac{2\xi}{w_n}p+1\right]}, \quad (2)$$

Where $k$ is constant term, $w_n$ is undamped natural frequency and $\xi$ is damping ratio.

It is even possible to obtain the transfer function under MATLAB in continuous time of each winding which is a mathematical representation of a linear time-invariant (LTI) system. It relates the Laplace transform of the output of the system to the Laplace transform of the input. The transfer function is denoted as *H(p)*, where '*p*' represents the complex variable in the Laplace domain.

The general form of a transfer function in continuous time is:

$$Z(p) = \frac{Y(p)}{X(p)}, \quad (3)$$

Where *Z(p)* is the transfer function, *Y(p)* is the Laplace transform of the output signal (response), and *X(p)* is the Laplace transform of the input signal (excitation).

The transfer function can be represented in different forms depending on the system. We have chosen to represent the windings of the motor under study as a continuous-time transfer function. This form is the ratio of two polynomials in '*p*'. In this way, the transfer function of the motor windings impedance can be written as:

$$Z(p) = \frac{(b_n\times p^n)+\ldots..(b_3\times p^3)+(b_2\times p^2)+(b_1\times p^1)+b_0}{(a_n\times p^n)+\ldots..(a_3\times p^3)+(a_2\times p^2)+(a_1\times p^1)+a_0}, \quad (4)$$

Where $b_n$ are the coefficients of the numerator polynomial and $a_n$ are the coefficients of the denominator polynomial.

The continuous-time transfer function of an electric motor *Z(p)* is a mathematical illustration of the link between an electric motor's input and output variables in the frequency domain. It defines how the motor's speed, torque, or other performance traits change in response to changes in supply voltage or other input factors.

# 3. RESULTS

## 3.1 Behavior of Motor Windings

In the present study, the measurement and modeling of each winding have been conducted separately. *Figures 2* illustrate the results of impedance modeling of the universal motor's armature winding in the differential mode, following the measurement (in magnitude and phase).

The impedance evolution depicted in *figure 2* indicates that the armature exhibits an inductive behavior up to a frequency of 10 kHz, after which it transitions to a capacitive behavior. These conclusions are supported by the observations of the phase angle's progression. Specifically, the phase angle of the armature winding impedance starts with a positive value, decreases as the frequency increases, and eventually reaches zero at 10 kHz. Beyond this frequency, the phase angle becomes negative.

The model proposed for armature winding is consistent with the measurements made over the entire frequency range studied (100 Hz- 1 MHz).

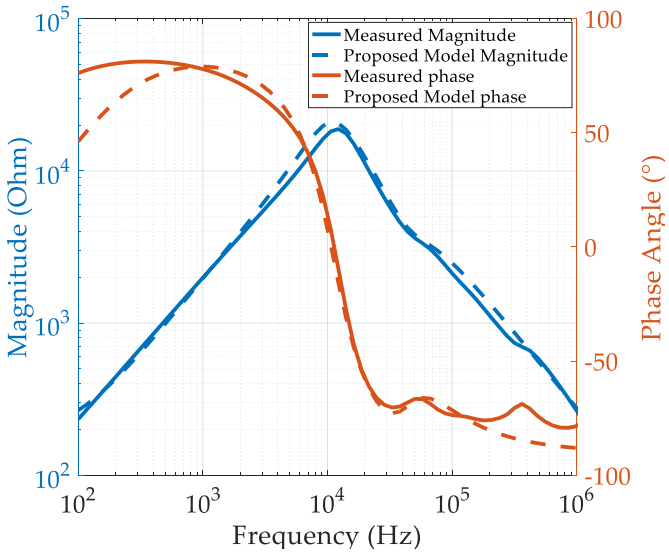


**Figure 2:** Impedance magnitude and phase of armature winding (DM)

The following formula provides the transfer function of the universal motor's armature winding impedance:

$$Z_A(p) = \frac{1.019\,10^{-9}p^3 + 4.484\,10^{-5}p^2 + 1.951\,p + 183}{3.687\,10^{-18}p^4 + 2.891\,10^{-13}p^3 + 1.122\,10^{-8}p^2 + 0.0001207\,p + 1}$$

The results of the measurement and simulation of the impedance (magnitude and phase) of the universal motor series winding are shown in *figure 3*.

It should be noted that the series winding behaves inductively up to 10 kHz. However, beyond this frequency, multiple slopes are observed, resulting in a behavior that is a combination of capacitive and inductive effects.

FOREX Publication
Open Access | Rapid and quality publishing
International Journal of Electrical and Electronics Research (IJEER)
Research Article | Volume 11, Issue 4 | Pages 1057-1064 | e-ISSN: 2347-470X

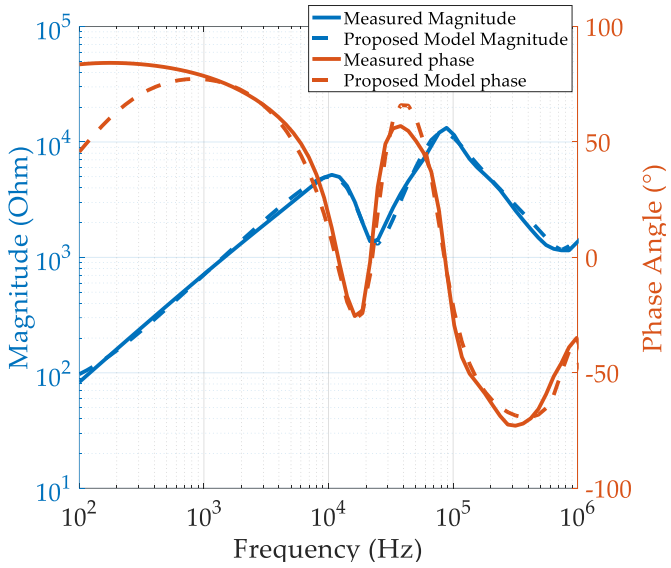


**Figure 3:** Impedance magnitude and phase of series winding (DM)

The transfer function of the series winding impedance of the universal motor is given by the following formula:

$$Z_S(p) = \frac{4.165\,10^{-36}p^8 + 5.42\,10^{-30}p^7 + 4.446\,10^{-24}p^6 + 2.342\,10^{-18}p^5 + 7.988\,10^{-14}p^4 + 3.193\,10^{-9}p^3 + 4.339\,10^{-5}p^2 + 0.7094\,p + 67}{2.535\,10^{-45}p^9 + 4.261\,10^{-39}p^8 + 4.409\,10^{-33}p^7 + 2.944\,10^{-27}p^6 + 3.185\,10^{-22}p^5 + 2.692\,10^{-17}p^4 + 9.814\,10^{-13}p^3 + 1.772\,10^{-8}p^2 + 0.0001902\,p + 1}$$

The measurement and simulation results for the impedance (magnitude and phase) of the universal motor compensating winding are shown in *figure 4*. The compensating winding's impedance is extremely comparable to that of a serial winding and exhibits inductive behavior up to 10 kHz. The impedance behavior shifts between capacitive and inductive after this frequency is exceeded, with numerous slopes observed up to 1MHz.

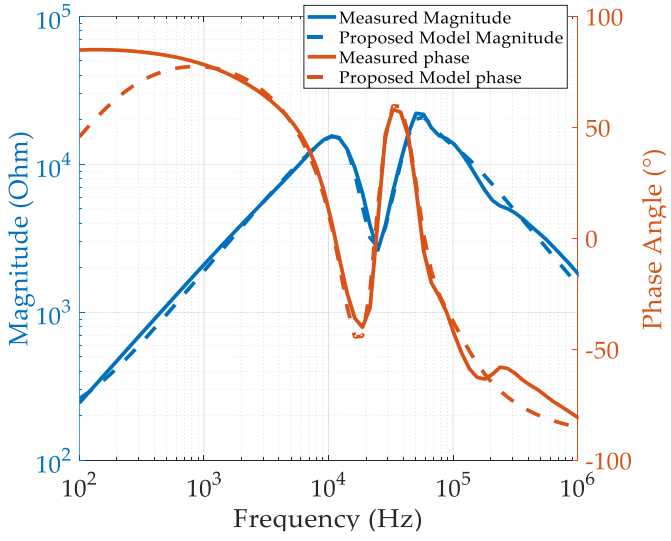


**Figure 4:** Impedance magnitude and phase of compensating winding (DM)

The universal motor compensation winding impedance's transfer function can be determined using the following formula:

$$Z_C(p) = \frac{2.926\,10^{-37}p^9 + 4.284\,10^{-32}p^8 + 5.167\,10^{-27}p^7 + 2.905\,10^{-22}p^6 + 1.524\,10^{-17}p^5 + 4.08\,10^{-13}p^4 + 1.108\,10^{-8}p^3 + 1.343\,10^{-4}p^2 + 1.907\,p + 180}{8.735\,10^{-47}p^{10} + 3.339\,10^{-41}p^9 + 5.941\,10^{-36}p^8 + 6.337\,10^{-31}p^7 + 4.459\,10^{-26}p^6 + 2.175\,10^{-21}p^5 + 7.479\,10^{-17}p^4 + 1.663\,10^{-12}p^3 + 2.331\,10^{-8}p^2 + 2.133\,10^{-4}p + 1}$$

## 3.2 UM Behaviour with and without Compensating

After analysing the frequency behaviour of each universal motor winding, the behaviour of the motor on the same frequency interval with and without compensation winding was studied. *Figure 5* represent the measurement and simulation results of the universal motor impedance (magnitude and phase) without compensation. We can see that the motor in this case has an inductive behavior up to frequency 10 kHz, beyond this frequency the behavior of the motor varies between capacitive and inductive.

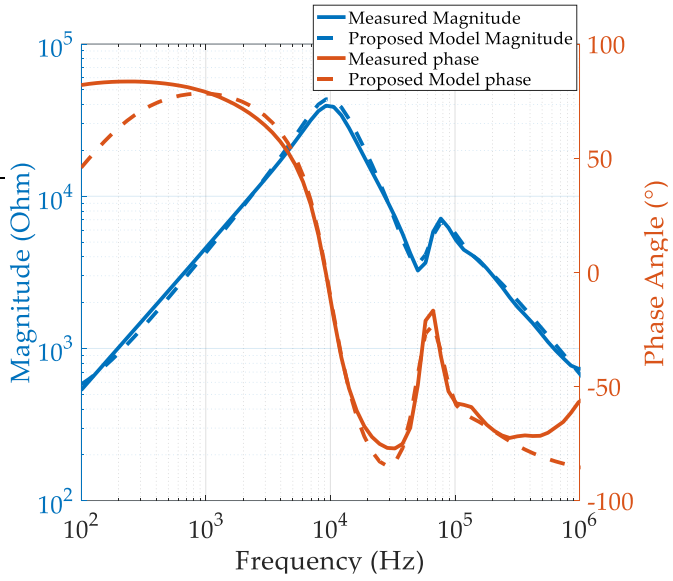


**Figure 5:** Impedance magnitude and phase of universal motor without compensating (DM)

The transfer function representing the impedance of the universal motor without compensation winding is given by the following formula:

$$Z_{AS}(p) = \frac{1.558\,10^{-38}p^9 + 3.323\,10^{-33}p^8 + 5.509\,10^{-28}p^7 + 5.243\,10^{-23}p^6 + 4.062\,10^{-18}p^5 + 2.084\,10^{-13}p^4 + 8.755\,10^{-9}p^3 + 2.172\,10^{-4}p^2 + 4.231\,p + 400}{2.27\,10^{-47}p^{10} + 6.686\,10^{-42}p^9 + 1.162\,10^{-36}p^8 + 1.347\,10^{-31}p^7 + 1.129\,10^{-26}p^6 + 6.988\,10^{-22}p^5 + 3.129\,10^{-17}p^4 + 9.821\,10^{-13}p^3 + 1.878\,10^{-8}p^2 + 1.598\,10^{-4}p + 1}$$

The behavior of the universal motor with a compensating winding is examined to conclude the study. The impedance (magnitude and phase) of the universal motor, measured and simulated with compensation, is shown in *figure 6*. It can be observed that the motor exhibits remarkably similar behavior in both setups, with and without compensation. The modeling results for the universal motor, with and without compensation,

FOREX Publication
Open Access | Rapid and quality publishing
International Journal of Electrical and Electronics Research (IJEER)
Research Article | Volume 11, Issue 4 | Pages 1057-1064 | e-ISSN: 2347-470X

are consistently good across the entire frequency range (100 Hz to 1 MHz).

Across the full frequency range, the modeling results of the universal motor with and without compensation are good (100 Hz-1 MHz).

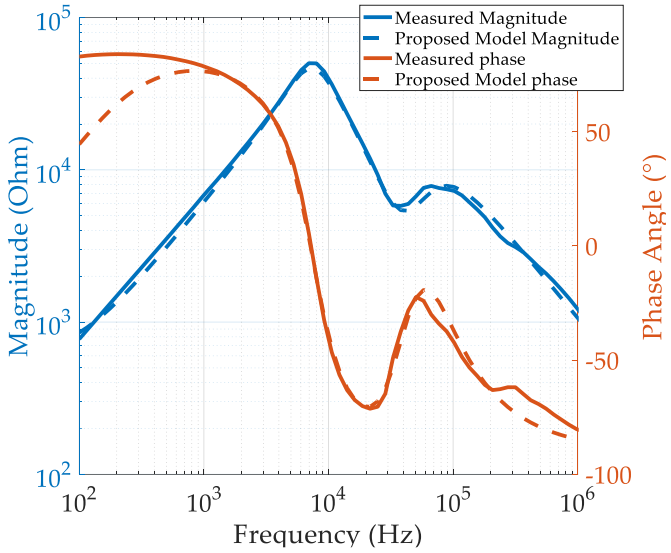


**Figure 6:** Impedance magnitude and phase of universal motor with compensating (DM)

Therefore, the following transfer function can be used to present the impedance of the universal motor with compensating winding:

$$Z_{ASC}(p) = \frac{2.467\ 10^{-18}\,p^5 + 2.191\ 10^{-13}\,p^4 + 1.261\ 10^{-8}\,p^3 + 3.443\ 10^{-4}\,p^2 + 6.095\,p + 600}{2.315\ 10^{-27}\,p^6 + 4.203\ 10^{-22}\,p^5 + 3.539\ 10^{-17}\,p^4 + 1.491\ 10^{-12}\,p^3 + 2.818\ 10^{-8}\,p^2 + 1.924\ 10^{-4}\,p + 1}$$

## 3.3 Correlation Analysis between Measurements and Model Prediction

In order to evaluate the predictive quality of the model used in this paper, the correlation between the impedance values measured and those proposed by the model used was studied. The cloud of points obtained is analyzed in relation to a linear regression line that has been drawn. It is also possible to calculate the correlation coefficient *r*, which can be used as a measure of a model's predictive accuracy. It shows the extent to which the model's predictions are in line with the actual values observed. The correlation coefficient $r$ between two variables $x$ and $y$ is calculated using the following formula:

$$r = \frac{n\sum xy - \left(\sum x \sum y\right)}{\sqrt{n\sum x^2 - \left(\sum x\right)^2} \times \sqrt{n\sum y^2 - \left(\sum y\right)^2}}, \quad (5)$$

Where $n$ is the number of data items. In our case, $x$ and $y$ represent respectively the values measured and those predicted by the model.

The coefficient of determination $R^2$ (the square of the linear correlation coefficient $r$) is an indicator used to judge the quality of a simple linear regression. It measures how well the model fits the observed data, or how well the regression equation describes the distribution of points.

In the example shown in the *figure 7* below, we have studied the linear regression of the proposed model compared with the measurements taken for the magnitude of the impedance of the universal motor with compensation (case of *figure 6*).

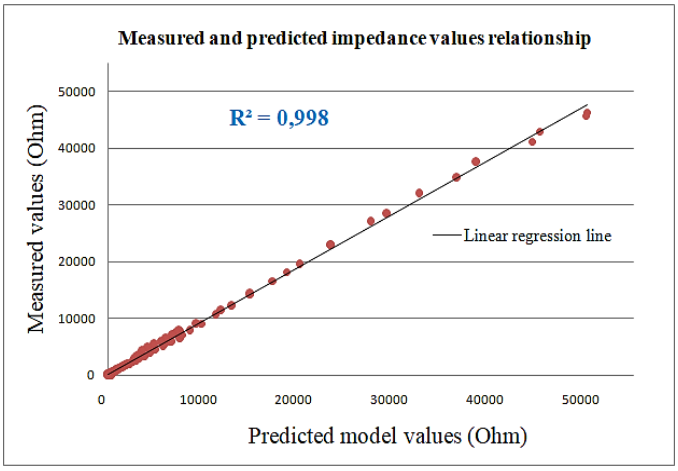


**Figure 7:** Correlation analysis between measured values and those predicted by the model

We can observe the alignment of the point cloud with the linear regression line. This suggests that the proposed model and the measurements have a strong positive correlation. This is supported by the close-to-1 values of correlation and determination coefficients that were attained ($r$ = 0.999 and $R^2$ = 0.998). In other words, the fact that the motor impedance values measured with the impedance analyzer and those predicted with transfer function modeling have a strong positive correlation means that the model proposed in this work offers excellent predictive quality.

## 3.4 Discussion

The transfer function modeling of the UM gave very satisfactory results over a wide frequency range. The correlation analysis between measurements and model predictions shows the excellent predictive quality of the proposed model for frequencies up to 1MHz.

### 3.4.1 Windings' effect on Universal Motor's EMC Performance

If we examine the universal motor's behavior in *figures 5* and *6*, we can observe a reduction in motor impedance for frequencies higher than 10 kHz, increasing the DM current. This may result in a motor overheating, deterioration of the insulation, and a shorter motor life. The armature winding's capacitive behavior, whose impedance is inversely proportional to frequency starting at 10 kHz (*figure 2*), can be used to explain this. These findings should motivate researchers and industry professionals to take into account practical methods for increasing the EMC effectiveness of universal motors from the earliest stages of their design, especially with regard to the armature winding

FOREX Publication
Open Access | Rapid and quality publishing
International Journal of Electrical and Electronics Research (IJEER)
Research Article | Volume 11, Issue 4 | Pages 1057-1064 | e-ISSN: 2347-470X

component, opening up options for additional study into the creation of more durable universal motors.

The series winding (*figure 3)* has an unstable impedance that can rise even at very high frequencies, in contrast to the armature. As a result, it is difficult to determine how this winding affects the EMC behavior of the motor; yet, it is evident that the armature winding is more electromagnetically noisy than the series winding.

The results of the universal motor with and without compensation may be compared (*figure 5* and *figure 6)*, and it can be shown that the motor impedance is larger with the compensation winding, lowering the DM current. This should encourage the designers of this type of motor to incorporate a compensation winding because it is plainly beneficial for EMC.

### 3.4.2 Circuit Model for Universal Motor Windings

If we examine the universal motor's behavior in *figures 5* and *6*, we can observe a reduction in motor impedance for frequencies higher than 10 kHz, increasing the DM current. This may result in a motor overheating, deterioration of the insulation, and a shorter motor life. The armature winding's capacitive behavior, whose impedance is inversely proportional to frequency starting at 10 kHz (*figure 2*), can be used to explain this. These findings should motivate researchers and industry professionals to take into account practical methods for increasing the EMC effectiveness of universal motors from the earliest stages of their design, especially with regard to the armature winding component, opening up options for additional study into the creation of more durable universal motors.

The series winding (*figure 3*) has an unstable impedance that can rise even at very high frequencies, in contrast to the armature. As a result, it is difficult to determine how this winding affects the EMC behavior of the motor; yet, it is evident that the armature winding is more electromagnetically noisy than the series winding.

The results of the universal motor with and without compensation may be compared (*figure 5 and figure 6*), and it can be shown that the motor impedance is larger with the compensation winding, lowering the DM current. This should encourage the designers of this type of motor to incorporate a compensation winding because it is plainly beneficial for EMC.

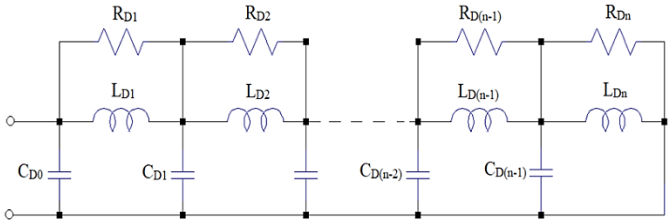


**Figure 8:** RLC multistage model circuit for universal motor windings in DM

The selected peaking and dipping frequencies are noted respectively (*fp1, fp2, ..., fpn*) and (*fd1, fd2, ..., fdn*). *Table 2* lists the different resonance frequency values that were chosen for every universal motor winding under study from the proposed high-frequency model, along with the number of stages for each winding's model circuit.

**Table 2: Peaking and dipping frequencies selected**

| Universal Motor's windings | Figures | Peaking and dipping frequencies (KHz) | | | | | | Model circuit stages number |
|---|---|---|---|---|---|---|---|---|
| | | fd1 | fp1 | fd2 | fp2 | fd3 | fp3 | |
| **Armature** | **Fig.2** | 12.24 | 43.7 | 76.93 | 316.3 | / | / | 02 |
| **Serie** | **Fig.3** | 12.24 | 24.82 | 88.61 | 156 | 238.4 | 738.9 | 03 |
| **Compensating** | **Fig.4** | 10.63 | 24.82 | 50.33 | 76.93 | 102.1 | 238.4 | 03 |
| **Armature + Serie** | **Fig.5** | 9.22 | 50.33 | 76.93 | 117.6 | 156 | 316.3 | 03 |
| **Armature + Serie + Compensating** | **Fig.6** | 8 | 32.93 | 57.98 | 274.6 | / | / | 02 |

Once the resonance frequencies selected and the number of RLC circuit stages for each winding has been established, the values for each component of the model circuit must be calculated. The parameterization of model circuits is outside the scope of this paper, but it might be a logical next step for further investigation.

Therefore, equivalent circuits for every winding of the universal DM motor up to 1MHz can be developed using the proposed model. Due to multiple resonance frequencies and the unstable winding impedance behavior for frequencies above 1MHz, the suggested model has certain limitations at higher frequencies.

## 4. CONCLUSION

The work presented in this paper was carried out in several stages:

The first is the practical measurement of the impedance of each motor winding in the first instance, and of the motor as a whole in the second, using an impedance analyzer.

The second part was designed to use the measurements to develop an HF behavioral model of the motor using the asymptotic Bode method under MATLAB programming software. We have proposed a behavioral model providing a better representation of the DM impedances of the universal

FOREX Publication
Open Access | Rapid and quality publishing
International Journal of Electrical and Electronics Research (IJEER)
Research Article | Volume 11, Issue 4 | Pages 1057-1064 | e-ISSN: 2347-470X

motor windings for high-frequency values up to 1MHz. The results obtained demonstrate the excellent predictive quality of the proposed model, which enables us to accurately predict the HF behavior of the universal motor and its windings in DM. Analysis of the results obtained has enabled us to study and understand the behavior and influence of each motor element on the impedance and therefore on the electromagnetic disturbance of the motor. Finally, a multi-stage RLC model circuit was proposed to represent each winding of the universal motor.

The EMC HF investigation of universal motors has been neglected, and the results obtained in this paper clearly indicate that this type of machine can be a source of electromagnetic disturbance, and provide some guidelines to follow in order to improve the performance and efficiency of this type of machine. The study presented in this paper opens the way to several interesting perspectives in the study of EMI in electrical machines:

- Using the transfer function modeling method to study the propagation of EMI in the common mode of the universal motor windings;
- Parameterization of the model circuits proposed for each winding;
- Extend the frequency study to 1 GHz;
- The modeling method used for the universal motor can be tested for other types of single-phase or three-phase electrical machines

**Author Contributions:**
Impedance Analyzer calibration: M. Miloudi and A. Gourbi; Acquisition of measurement data: M.H. Bermaki and H. Miloudi; Matlab software programming: H. Miloudi; Modeling: M.H. Bermaki; Interpretation of results: M.H. Bermaki; Article drafting: M.H. Bermaki, H. Miloudi and A. Bendaoud; Supervision: A. Bendaoud. All authors have read and agreed to the published version of the manuscript.

**Funding:**
This research was funded by the Ministry of Higher Education and Scientific Research (Algeria) through the PRFU research project with the code: A01L07UN220120220004

**Conflicts of Interest:**
The authors declare no conflict of interest.

## REFERENCES

[1] S. W. Shneen, A. L. Shuraiji, K. R. Hameed. Simulation model of proportional integral controller-PWM DC-DC power converter for DC motor using MATLAB. IJEECS 2023, Vol. 29, No. 2, pp. 725-734.

[2] Y. Özüpak. Investigation of the Effect of Design Parameters of Small Brushless DC Motors on Motor Performance by Finite Element Method. BEN 2022, Vol. 3, p. 4658.

[3] K. A. Abro, A. Atangana, J.F. Gómez-Aguilar. Chaos control and characterization of brushless DC motor via integral and differential fractal-fractional techniques. IJMS 2022, Vol. 43, No. 4, pp. 416-425.

[4] I. A. Araga, A. E. Airoboman, A. P. Inalegwu, I. A. Afolayan, F. O. Adunola. A comparative analysis on the performance of universal motor when driven by alternating current/direct current. AJST 2020, Vol. 4, No. 4, pp. 348-352.

[5] S. Andi, W. Widjonarko, K. Candrika. Synchronous AC Chopper for Universal Motor Speed Control Using Fuzzy Logic. FESPE 2021, Vol. 3, No. 2, pp. 13-24.

[6] S. K. Sharma and M. S. Manna. Finite Element Electromagnetic Based Design of Universal Motor for Agro Application. IJEER 2022, Vol. 10, Issue. 3, pp. 590-596.

[7] P. Girovský, J Kaňuch, "Analysis of the Power Supply Influence on the Universal Motor", PEAD 2022, Vol. 7, No 1, pp. 103-111.

[8] H. QI, L. Ling, C. Jichao, X. Wei. Design and research of deep slot universal motor for electric power tools. JPE 2020, Vol. 20, No. 6, pp. 1604-1615.

[9] D. S. Nayak, R. Shivarudraswamy. Efficiency and loss analysis of proposed BLDC motor drive and existing universal motor drive used in a mixer grinder. IJMERR 2020, Vol. 9, No. 6, pp. 808-812.

[10] A. Mercy, B. Umamaheswari, K. Latha. Reduced-order thermal behavior of universal motor-driven domestic food mixers/grinders using AC and DC supplies. JPE 2021, Vol. 21, pp. 1322-1332.

[11] K. Kurihara, S Koseki. New design of high output equivalent 4-pole universal motor. XIII International Conference on Electrical Machines (ICEM), Alexandroupoli, Greece, September 2018, IEEE, pp. 291-296.

[12] V. Umesh, S. Mishra, S. Simon, A. K. Singh, P. Moses. Universal electrical motor acoustic noise reduction based on rotor surface modification. International Conference on Data Science and Communication (IconDSC), Bangalore, India, March 2019, IEEE, pp. 1-5.

[13] L. Xheladini, A. TAP, T. AŞAN, M. Yilmaz. Permanent Magnet Synhronous Motor and Universal Motor comparison for washing machine application. 11th IEEE International Conference on Compatibility, Power Electronics and Power Engineering (CPE-Powereng), Cadix, Spain, April 2017, IEEE, pp. 381-386.

[14] Y. Moreno, G. Almandoz, A. Egea, B. Arribas. Analysis of permanent magnet motors in high frequency—a review. Appl. Sci. 2021, Vol. 11, No. 14, pp. 6334.

[15] M. Karthik, S. Usha, K. Venkateswaran, H. Panchal, M. Suresh, V. Priya, K. K. Hinduja. Evaluation of electromagnetic intrusion in brushless DC motor drive for electric vehicle applications with manifestation of mitigating the electromagnetic interference. Int. J. of Ambient Energy, 2020, pp. 1-8.

[16] V. Karakaşli, F. Gross, T. Braun, H. De Gersem, G. Griepentrog. High-frequency modeling of delta-and star-connected induction motors. IEEE Trans. Electromagn. 2022, Vol. 64, No. 5, pp. 1533-1544.

[17] J. Park, S. Park, K. H. Jung, I. J. Yoon. High-frequency Modeling of a BLDC Motor for Radiated Emission Prediction. IEEE International Symposium on Electromagnetic Compatibility & Signal/Power Integrity (EMCSI), Glasgow, Scotland, July 2021, IEEE, pp. 523-523.

[18] Z. Zhao, F. Fan, Q. Sun, P. Tu. High-frequency modeling of induction motor using multilayer perceptron. Asia-Pacific International Symposium on Electromagnetic Compatibility (APEMC), Beijing, China, September 2022, IEEE, pp. 222-224.

[19] B. Mirafzal, G. L. Skibinski, R. M. Tallam, D. W. Schlegel, R. A. Lukaszewski. Universal induction motor model with low-to-high frequency-response characteristics. IEEE Trans. Ind. Appl. 2007, Vol. 43, No. 5, pp. 1233-1246.

[20] H. Miloudi, M. Miloudi, A. Gourbi, M. H. Bermaki, A. Bendaoud. A high-frequency modeling of AC motor in a frequency range from 40 Hz to 110 MHz. Electrical Engineering & Electromechanics 2022, No. 6, pp. 3-7.

[21] H. Miloudi, A, Bendaoud, M. Miloudi, S. Dickmann, S. Schenke. A novel method of transfer-function identification for modeling DM impedance of AC motor. International Symposium on Electromagnetic Compatibility-EMC Europe, Angers, France, September 2017, IEEE, pp. 1-5.

[22] J. Sun and L. Xing. Parameterization of Three-Phase Electric Machine Models for EMI Simulation. IEEE Transactions on Power Electronics 2014, vol. 29, No. 1, pp. 36-41.

Open Access | Rapid and quality publishing

International Journal of
Electrical and Electronics Research (IJEER)
Research Article | Volume 11, Issue 4 | Pages 1057-1064 | e-ISSN: 2347-470X

[23] Y. Moreno, G. Almandoz, A. Egea, B. Arribas, A. Urdangarin. Analysis of permanent magnet motors in high frequency—a review. Applied Sciences 2021, vol. 11, No. 14, p. 6334.